A Pseudospectral Model for Dispersion of Atmospheric Pollutants

OVE CHRISTENSEN[1] AND LARS P. PRAHM

Danish Meteorological Institute, DK-2100 Copenhagen ø, Denmark

(Manuscript received 7 April 1976)

ABSTRACT

An Eulerian model, describing the dispersion of pollutants in gases and fluids, is developed. The model is based on numerical integration of the dispersion equation, including the effect of advection, diffusion, sinks and of multiple sources. The pseudospectral method is employed for numerical integration of the dispersion equation. The model is not limited to physical problems with periodic boundary conditions, as imposed by the spectral technique. A filtering procedure prevents instabilities caused by aliasing interactions. The emphasis is placed on numerical tests relevant to air pollution studies. Pseudodiffusion is not present in this model. The error in numerical integration is brought down to a few percent of the concentration level of the pollutant. To our knowledge, the model is the most accurate Eulerian model presently available for dispersion calculations. Applications to air pollution studies are discussed. Accuracy of 19 different numerical methods is compared.

1. Introduction

Numerical modeling of air pollution dispersion is of increasing importance in the study of various aspects of air pollution. Models have applications as a tool for:

- Interpretation of measured air quality data
- Surveillance of air quality in combination with on-line measurements
- Prognostic analysis of air quality subject to different estimated emission patterns and meteorological conditions
- The study of the basic physical conditions describing the dispersion of atmospheric pollutants (Egan and Mahoney, 1972b).

Numerical models rely on the input data, the mathematical formulation of the chemical and physical processes, and on the accuracy of the numerical schemes. In this work we present an improved numerical method in which numerical truncation errors are reduced to a few percent of the concentration level of the pollutant.

Time-dependent flows in the atmosphere can be treated by different numerical methods based on either Eulerian or Lagrangian formulations. In the Eulerian formulation the concentration of the pollutant refers to a coordinate system fixed in space through which the air is moving. In the Lagrangian formulation the concentration variables refer to a coordinate system fixed in relation to the mean flow of air.

Some Lagrangian puff models for single-point sources (Sheih and Moroz, 1973; Start and Wendell, 1974) are able to account for atmospheric inhomogeneities with a length scale larger than the dimensions of the puff. A multiple source Lagrangian model was developed for regional dispersion computations by Eliassen and Saltbones (1975a). In this model the Lagrangian coordinate system had to be regenerated when distorted to such a degree that individual trajectories cross each other. The existing puff models seem unable to account for the detailed structure in the atmospheric boundary layer, and the multiple-source Lagrangian model has no control on the numerical truncation errors involved in the method.

Hybrids of Eulerian and Lagrangian techniques such as the Particle In Cell (PIC) and the moment method have been developed. The PIC method (Sklarew *et al.*, 1971) is based on a number of Lagrangian particles within each cell. Each particle represents a discrete amount of the pollutant, and its position is computed at every time step. A large number of particles is necessary to obtain a low level of truncation error. Pseudodiffusion caused by the numerical advection is avoided. The method has advantages and drawbacks common to Lagrangian methods in general. The moment method was suggested by Egan and Mahoney (1972a), and a test of the numerical truncation errors in two dimensions is given by Pedersen and Prahm (1974). The method is based on computation of the first- and second-order moment of mass with respect to position in each cell. As in the PIC method this method has reduced the truncation error to an acceptable level for many atmospheric dispersion computations and gives possibilities for subgrid-scale information to be represented such as point source emissions.

[1] Present affiliation: Institute of Medical Physiology A, University of Copenhagen.

Because of the direct connection to source and deposition coordinates the Eulerian methods are in general preferable for numerical integration of the dispersion equation. However, none of the existing Eulerian dispersion models appear to have numerical errors less than 10% after flow through a space-grid system in a uniform circular velocity field.

The problem of the stability of Eulerian numerical schemes has received a great deal of attention from researchers in applied mathematics. The accuracy of the numerical scheme has just recently received similar attention (Molenkamp, 1968; Crowley, 1968; Orszag, 1971a; Anderson and Fattahi, 1974; Pedersen and Prahm, 1974), and it is shown that the accuracy of a great deal of commonly used lower order finite difference schemes are inadequate for many applications. Numerical integration techniques based on a cutoff expansion of the concentration in orthogonal functions have recently been shown to be very accurate. These techniques are the Galerkin (spectral) method (Orszag, 1971a) and the pseudospectral method (Gazdag, 1973; Fox and Orszag, 1973).

Inspired by these results we develop and test in this study the first pseudospectral model with emphasis on practical application for atmospheric dispersion computations. The major restriction of the pseudospectral method is the presence of periodic boundary conditions. In the present work we have found a simple way of overriding these conditions. The final model combines the high accuracy and computational speed of the spectral methods, using fast Fourier transformation, without the restriction of periodic boundary conditions. With respect to computational time and space the model is now to the authors' knowledge the most accurate existing multiple-source Eulerian model for practical dispersion computations in fluids and gases.

Despite the obvious possibility for accurate solution of the atmospheric diffusion equation by spectral methods, this approach has not been applied until now. Lack of experience with Fourier space operations among air pollution meteorologists and modelers might be the reason. Therefore, a fairly detailed mathematical description of the methods developed is given in this paper.

2. The dispersion equation

Most air pollution dispersion computations are based on the semi-empirical gradient transfer theory (Monin and Yaglom, 1971). In this approach the concentration of pollutant, $c(\bar{\mathbf{x}},t)$, is governed by the dispersion equation

$$\frac{\partial c}{\partial t}=-\nabla\cdot(\bar{\mathbf{v}}c)+\nabla\cdot(D\nabla c)+Q+S, \tag{1}$$

where $\bar{\mathbf{v}}$ is the wind velocity and D the eddy diffusion constant. Q and S represent sources and sinks, respectively; S, Q, D and $\bar{\mathbf{v}}$ are external variables in space and time. The first term on the right-hand side of (1) describes advection and the second term describes eddy diffusion. Assuming an incompressible velocity field, the equation can be written as

$$\frac{\partial c}{\partial t}=-(\bar{\mathbf{v}}-\nabla D)\cdot\nabla c+D\nabla^2 c+Q+S. \tag{2}$$

It is noteworthy that the term $-\nabla D$ acts as a "diffusion wind" which contributes to the advection. The source term Q includes multiple sources and the drain (or sink) term S describes the effect of chemical processes as well as dry and wet deposition.

Comparison between empirical data and solutions to (1) has only been performed in simplified cases as no general solution to the equation has been worked out in three space dimensions. The basic limitations of the gradient transfer theory for turbulent diffusion are discussed by Monin and Yaglom (1971), and by Pasquill (1974). Only eddies with characteristic dimensions smaller than the extension of a considered plume can be represented by a constant diffusion constant. At larger distances from point sources the theory agrees with the result of a purely statistical treatment (Taylor, 1921), while discrepancy between empirical data and the gradient transfer theory is found for diffusion times smaller than the Lagrangian time scale. The range of applicability of models based on a solution of (1) is thus typically limited to distances larger than a few kilometers.

3. Numerical method

a. The pseudospectral approximation

In order to obtain a numerical solution to the dispersion equation (2) we shall employ the pseudospectral, or collocation, approximation. In this approximation, the space derivatives on the right-hand side of (2) are computed by means of finite Fourier transforms, that is, in spectral space, whereas the local products and the time integration are evaluated in physical space.

We shall assume that values of concentration and of external variables are specified on a two-dimensional mesh of size $N_1\times N_2$. Extension to more than two dimensions is trivial. The location of a mesh point is given by the vector $\bar{\mathbf{x}}=(x_1,x_2)$ where

$$x_i=\Delta x_i m_i, \quad m_i=0, 1, \ldots, N_i-1, \tag{3}$$

where Δx_i is the spacing between mesh points. The value of the concentration on such a point is $c(\bar{\mathbf{x}},t)$. The finite Fourier expansion of the concentration is given by

$$c(\bar{\mathbf{x}},t)=\sum_{\bar{\mathbf{k}}} A(\bar{\mathbf{k}},t)\exp(i\bar{\mathbf{k}}\cdot\bar{\mathbf{x}}). \tag{4}$$

The range of $\bar{\mathbf{k}}$ values in the summation is determined

from $\bar{\mathbf{k}}=(k_1,k_2)$ with

$$k_i=\frac{2\pi}{\Delta x_i N_i}n_i, \tag{5}$$

where n_i assumes integer values within the limits $-N_i/2<n_i\leqslant N_i/2$. Thus $-K_i<k_i\leqslant K_i$ with $K_i=\pi/\Delta x_i$ which we for short shall denote $-\bar{\mathbf{K}}<\bar{\mathbf{k}}\leqslant\bar{\mathbf{K}}$. With an expression from solid state physics, we say that $\bar{\mathbf{k}}$ belongs to the first Brillouin zone (BZ). The $\bar{\mathbf{k}}$ values are obtained from the requirement of periodic boundary conditions, i.e., that $c(x_1,x_2+\Delta x_2 N_2)=c(x_1,x_2)$ and similar for the other space variable. The maximum value of a wave vector component in (5) is K_i which corresponds to a wavelength of $2\Delta x_i$. The Fourier component $A(\bar{\mathbf{k}},t)$ in (4) is given by the finite Fourier Transform (FT)

$$A(\bar{\mathbf{k}},t)=\frac{1}{N_1N_2}\sum_{\bar{\mathbf{x}}}c(\bar{\mathbf{x}},t)\exp(-i\bar{\mathbf{k}}\cdot\bar{\mathbf{x}}), \tag{6}$$

where the $\bar{\mathbf{x}}$ summation is over all mesh-points. The space derivatives appearing on the right-hand side of (2) can now be evaluated on grid points using (4):

$$\frac{\partial c(\bar{\mathbf{x}},t)}{\partial x_j}=\sum_{\bar{\mathbf{k}}}ik_jA(\bar{\mathbf{k}},t)\exp(i\bar{\mathbf{k}}\cdot\bar{\mathbf{x}}), \tag{7}$$

$$\nabla^2c(\bar{\mathbf{x}},t)=\sum_{\bar{\mathbf{k}}}-k^2A(\bar{\mathbf{k}},t)\exp(i\bar{\mathbf{k}}\cdot\bar{\mathbf{x}}). \tag{8}$$

Thus in order to compute $\partial c/\partial x_j$ we first determine $A(\bar{\mathbf{k}},t)$ from the finite FT (6). $A(\bar{\mathbf{k}},t)$ is then multiplied by ik_j and $\partial c/\partial x_j$ can be determined by applying the inverse FT (4). In order to determine $\partial c/\partial x_1$, $\partial c/\partial x_2$ and $\nabla^2 c$ we then perform one FT, multiply by the proper wave vector factor and perform three inverse FT's. A total of four FT's is therefore required each time we compute the right-hand side of Eq. (2). The "diffusion wind" $-\nabla D$ can be calculated in the same manner as ∇c. For a given set of external parameters this can be done in the initialization procedure and does therefore not contribute significantly to the computation time.

b. *Advantages and drawbacks in the pseudospectral approximation*

The main advantage in the evaluation of space derivatives by the Fourier transform method is that the space derivatives are accurate within the limits which $c(\bar{\mathbf{x}},t)$ can be defined on the set of grid points $\bar{\mathbf{x}}$. The derivative at a grid point is derived from function values on all grid points. The derivatives obtained in this way are, however, by no means unique. If in Eq. (4) we use another set of orthogonal functions in place of $\exp(i\bar{\mathbf{k}}\cdot\bar{\mathbf{x}})$ the space derivatives would generally be different. Our reason for expanding $c(\bar{\mathbf{x}},t)$ in the set of orthogonal functions $\exp(i\bar{\mathbf{k}}\cdot\bar{\mathbf{x}})$ is the availability of the fast Fourier transform algorithm (Cooley and Tukey, 1965) which makes it possible to compute the space derivatives in a modest amount of time.

In the expressions for the space derivatives [(7) and (8)] an assumption is implicitly made about the behaviour of $c(\bar{\mathbf{x}},t)$ between grid points. Let us define the continuous space variable $\bar{\mathbf{x}}_c$ in the range $0\leqslant x_{ci}<\Delta x_i N_i$. Eqs. (7) and (8) imply that between grid points, $c(\bar{\mathbf{x}},t)$ is given by

$$c(\bar{\mathbf{x}}_c,t)=\sum_{\bar{\mathbf{k}}}A(\mathbf{k},t)\exp(i\bar{\mathbf{k}}\cdot\bar{\mathbf{x}}_c). \tag{9}$$

For a given continuous function $f(\bar{\mathbf{x}}_c,t)$ we can always determine $A(\bar{\mathbf{k}},t)$ from Eq. (6) such that $c(\bar{\mathbf{x}},t)=f(\bar{\mathbf{x}},t)$ on grid points. Between grid points $c(\bar{\mathbf{x}}_c,t)$ will in general differ from $f(\bar{\mathbf{x}}_c,t)$. The more Fourier components we use in the representation of $c(\bar{\mathbf{x}},t)$, i.e., the more mesh points we use, the better will the function $c(\bar{\mathbf{x}}_c,t)$ approximate $f(\bar{\mathbf{x}}_c,t)$. We shall omit here a discussion of the convergence properties of cutoff Fourier expansions. Such a discussion is given by Galerkin (1915), Lanczos (1957) and Orszag (1971a).

Orszag (1971a) shows that spectral methods are superior in accuracy to finite difference schemes on a given size of grid mesh but more time consuming. If for some problem a given accuracy is wanted, the spectral methods are, however, less time consuming than finite difference methods because a larger mesh will be needed in the finite difference methods in order to obtain the desired accuracy.

c. *Periodic boundary conditions*

The periodicity of $c(\bar{\mathbf{x}},t)$ present in the pseudospectral approximation is a consequence of the periodic boundary conditions which are necessary in order to make the expansions (4) and (6). Physically this means that a distribution $c(\bar{\mathbf{x}},t)$ which is advected out over one boundary appears again on the opposite boundary.

In order to avoid this we shall sacrifice information from the two outermost row and column grid points and let the concentration of the pollutant decay exponentially in these grid points, to be referred to as the boundary. Starting with, say, a 16×16 mesh we shall thus only use information from a 12×12 mesh.

In order to prevent difficulties from outflow conditions we add in (1) a drain term of the form $-c(\bar{\mathbf{x}},t)/\tau(\bar{\mathbf{x}})$. The decay constant $\tau(\bar{\mathbf{x}})$ assumes realistic values appropriate to the physical problems on the 12×12 mesh. If no decay is present here, we just assign a sufficiently large value to τ. On the boundary gridpoints we let τ assume a value so that the effective decay length is approximately equal to the grid spacing perpendicular to the boundary $\Delta x_\perp$. Thus for the perpendicular component of ∇c we demand

$$\nabla_\perp c\approx-\frac{c}{\Delta x_\perp}. \tag{10}$$

Apart from this condition we require that pollutant advected to the boundary should disappear here or, in other words, that $\partial c/\partial t$ should vanish at the boundary. This requirement yields

$$\tau(\bar{\mathbf{x}}) \approx \Delta x_\perp / v_\perp(\bar{\mathbf{x}}), \tag{11}$$

where $v_\perp(\bar{\mathbf{x}})$ is the component of velocity perpendicular to the boundary. This is under the assumption that the main contribution to $\partial c/\partial t$ is due to the advection term rather than to diffusion. We shall later show that this condition is fulfilled for air pollution modeling on a mesoscale and a regional scale. In the case of strong diffusion (which is not tested here) we suggest using a value of τ given by

$$\frac{1}{\tau(\bar{x})} \approx \frac{v_\perp}{\Delta x_\perp} + \frac{D(\bar{x})}{\Delta x_\perp{}^2}. \tag{12}$$

The strong gradient created at the boundary gives rise to out-diffusion here. This can be handled by setting $D(\bar{\mathbf{x}})=0$ at the boundary. The term $-\nabla D$ should then be included in the velocity. This term has rather poor convergence properties (Lanczos, 1957) and a sigma filtering is advisable (Lanczos, 1957). In practice we found that for values of the diffusion constant relevant on a mesoscale and a regional scale omission of the ∇D term created only minor errors. In modeling of air pollution dispersion one would probably use local values of D and the term would have to be taken into account.

d. Aliasing errors and the filtering technique

In order to comply with realistic outflow conditions, we have introduced space-dependent values of $\tau(\bar{\mathbf{x}})$ and $D(\bar{\mathbf{x}})$. On the right-hand side of (2) there are now three terms which contain the product of $c(\bar{\mathbf{x}},t)$ or its derivatives with a space-dependent variable, i.e., with $\bar{\mathbf{v}}(\bar{\mathbf{x}})$, $D(\bar{\mathbf{x}})$ and with $1/\tau(\bar{\mathbf{x}})$. We shall in the following consider the so-called aliasing error introduced by these "nonlinear" products. Aliasing errors arise because the grid system cannot resolve wavelengths shorter than about two grid intervals (Phillips, 1959). Such wavelengths are formed by the nonlinear interaction of the longer wavelengths contained in each of the factors in the products appearing on the right-hand side of (2). The grid system interpretes these wavelengths incorrectly as long waves.

As a simple example we consider the product $p(\bar{\mathbf{x}})$ of two functions $a(\bar{\mathbf{x}})$ and $b(\bar{\mathbf{x}})$ defined on the mesh of grid points (3). Application of Eq. (4) yields

$$\left.\begin{aligned} a(\bar{\mathbf{x}}) &= \sum_{\bar{k}_a} A(\bar{\mathbf{k}}_a)\exp(i\bar{\mathbf{k}}_a\cdot\bar{\mathbf{x}}) \\ b(\bar{\mathbf{x}}) &= \sum_{\bar{k}_b} B(\bar{\mathbf{k}}_b)\exp(i\bar{\mathbf{k}}_b\cdot\bar{\mathbf{x}}) \end{aligned}\right\}, \quad -\bar{\mathbf{K}}<\bar{\mathbf{k}}_a,\bar{\mathbf{k}}_b\leqslant\bar{\mathbf{K}}.$$

The product will thus contain terms like

$$A(\bar{\mathbf{k}}_a)\cdot B(\bar{\mathbf{k}}_b)\exp[i(\bar{\mathbf{k}}_a+\bar{\mathbf{k}}_b)\cdot\bar{\mathbf{x}}],$$

where in general $-2\bar{\mathbf{K}}<\bar{\mathbf{k}}_a+\bar{\mathbf{k}}_b\leqslant 2\bar{\mathbf{K}}$. A product term for which $\bar{\mathbf{K}}<\bar{\mathbf{k}}_a+\bar{\mathbf{k}}_b<2\bar{\mathbf{K}}$ will on the grid system (3) be represented as having a wave vector $\bar{\mathbf{k}}_a+\bar{\mathbf{k}}_b-2\bar{\mathbf{K}}$ which belongs to the first BZ. We have here used the periodicity of the Fourier components in spectral space i.e., $A(\bar{\mathbf{k}})=A(\bar{\mathbf{k}}-2\bar{\mathbf{K}})$. The corresponding Fourier component of the gradient of the product will thus be $i(\bar{\mathbf{k}}_a+\bar{\mathbf{k}}_b-2\bar{\mathbf{K}})A(\bar{\mathbf{k}}_a)B(\bar{\mathbf{k}}_b)$ instead of $i(\bar{\mathbf{k}}_a+\bar{\mathbf{k}}_b)A(\bar{\mathbf{k}}_a)\times B(\bar{\mathbf{k}}_b)$. This leads to errors in the space derivatives.

Orszag (1971a,b) has pointed out that aliasing errors can be removed by only retaining terms in $p(\bar{\mathbf{x}})$ for which $\bar{\mathbf{k}}_a+\bar{\mathbf{k}}_b$ belongs to the first BZ. In order to obtain an alias free product, Orszag (1971b) has developed a transform method which removes instabilities caused by aliasing interactions. In the applications of the pseudo-spectral approximation to air pollution dispersion it is more important to reach a result with say 10% typical error in short time than to reach a result with 1% error in an immoderately long time. Use of Orszag's transform method here would increase computation time typically by a factor of 3–4. We shall therefore look for more simple ways of removing aliasing interactions at the expense of some accuracy and with some loss of generality.

Our approach is based on the assumption that $\bar{\mathbf{v}}(\bar{\mathbf{x}})$, $D(\bar{\mathbf{x}})$ and $1/\tau(\bar{\mathbf{x}})$ are fairly slowly varying quantities on the grid. More specifically, we assume that these quantities essentially can be represented by fairly longwave Fourier components. This will usually be the case for the velocity field $\bar{\mathbf{v}}(\bar{\mathbf{x}})$ and our results obtained with the choice made for $1/\tau(\bar{\mathbf{x}})$ and $D(\bar{\mathbf{x}})$ indicate that these variables fulfil the requirement, too. Thus we assume that the three above mentioned quantities have "large" Fourier components only in a region of Fourier space given by $|\bar{\mathbf{k}}|\leqslant k_f$. On a square mesh we approximate $c(\bar{\mathbf{x}},t)$ by the function

$$c_F(\bar{\mathbf{x}},t)=\sum_{|\bar{k}|<K_f} A(\bar{\mathbf{k}},t)\exp(i\bar{\mathbf{k}}\cdot\bar{\mathbf{x}}), \tag{13}$$

which is obtained from $c(\bar{\mathbf{x}},t)$ by letting $A(\bar{\mathbf{k}})=0$ for $|\bar{\mathbf{k}}|>K_f$, that is, by passing $c(\bar{\mathbf{x}},t)$ through a low-pass filter with an abrupt cutoff at K_f. Usually we used $K_f=K_1=K_2$. We have not tested cases where $\Delta x_1\neq\Delta x_2$. In this case we would suggest replacing the circle of radius K_f by an ellipse with axes K_1 and K_2. Obviously an error is introduced by replacing $c(\bar{\mathbf{x}},t)$ by $c_F(\bar{\mathbf{x}},t)$. As we shall demonstrate later, this error is in most cases so small that it does not significantly alter the result. Even more important is that this error is known *ab initio*.

The idea is now that aliasing terms between $c_F(\bar{\mathbf{x}},t)$ and the three space variables will appear in the "empty" part of the first BZ where $|\bar{\mathbf{k}}|>K_f$. We shall call this region the aliasing zone. The product terms will contain Fourier components out to a maximum wave vector length of k_f+K_f. Thus a large fraction of the aliasing terms produced will have wave vectors in the aliasing

zone. Wave vectors outside the first BZ will through aliasing be shifted to wave vectors like $\bar{\mathbf{k}}-2\bar{\mathbf{K}}$ and mainly end up in the aliasing zone. After several time steps the aliasing terms produces new aliasing terms, etc. However, before such a term effectively enters the zone $|\bar{\mathbf{k}}| \leqslant K_f$ we apply a new filtering to $c_F(\bar{\mathbf{x}},t)$, thereby clearing the aliasing zone. In practice, filtering was done at regular intervals corresponding to advection a distance of the order of a typical distance unit in the particular problem considered. The use of filtering increased the computational time typically 5–10%.

e. *Time-integration procedure*

The time-integration procedure used in the numerical tests was the leap-frog or midpoint-rule integration. For pure advection problems this is a stable integration procedure. Under such conditions the errors from time integration were negligible when on a square mesh the time step was chosen such that $\Delta t\, v_{\max} \leqslant 0.1\Delta x$, where $v_{\max}$ is the maximum absolute value of the velocity. With a non-zero value of the diffusion constant the leap-frog method is unstable (Lambert, 1973). It was found, however, that the filtering technique introduced to reduce aliasing errors at the same time eliminated the instability present in time integration. This gives no guarantee, of course, that instabilities from time integration might not evolve, but merely shows that in our numerical tests they did not appear. One is, of course, not bound to perform time integration by the leap-frog method. A higher order explicit linear multi-step procedure might prove economical.

f. *Summary*

The basic new feature in this paper is that of making the highly accurate pseudospectral method applicable to problems whose *physical* boundary conditions are non-periodic. These conditions are met by introducing a decay of the outflowing concentration at the boundary grid points. The rather harsh procedure used in doing so introduces aliasing errors. These errors are suppressed by a filtering technique. The cost of this is first a minor loss in accuracy; second, a loss of generality through the conditions imposed on the velocity field $\bar{\mathbf{v}}(\bar{\mathbf{x}})$, the diffusion constant $D(\bar{\mathbf{x}})$ and the decay time $\tau(\bar{\mathbf{x}})$; and third, although the filtering method has prevented aliasing errors in the numerical tests presented in the following section, there is no guarantee that aliasing instabilities might not eventually occur, owing to the approximate nature of the method. These restrictions will be shown in the following sections to have little or no effect on actual modeling of air pollution dispersion.

4. Numerical results

All computations are performed in single precision Fortran IV algorithms on an IBM 370/165 computer (Christensen and Prahm, 1976). Here we have for graphical convenience chosen a 16×16 grid mesh. Higher accuracy is obtainable on larger grids (Orszag, 1971a), but it turns out that sufficient accuracy in many cases can be achieved on the 16×16 grid. The two outermost row and column grid points are used to introduce the drain term described in the previous section. Values of $c(\bar{\mathbf{x}},t)$ on these points are left out of the results pre-

a

	3	4	5	6	7	8	9	10	11	12	13	14
3	-11		-21		13	27	13		-21		-11	
4				12	-15	-35	-15	12				
5	-21			-28	15	46	15	-28			-21	
6		12	-28	42		-68		42	-28	12		
7	13	-15	15		-57	144	-57		15	-15	13	-30
8	27	-35	46	-68	144	762	144	-68	46	-35	27	
9	13	-15	15		-57	144	-57		15	-15	13	-30
10		12	-28	42		-68		42	-28	12		
11	-21			-28	15	46	15	-28			-21	
12				12	-15	-35	-15	12				12
13	-11		-21		13	27	13		-21		-11	
14		12			-30		-30			12		

b

	3	4	5	6	7	8	9	10	11	12	13	14
3												
4			-10		14	-10	-10	14		-10		
5		-10	16		-16	11	11	-16		16	-10	
6					23	-13	-13	23				
7		14	-16	23	-27	13	13	-27	23	-16	14	
8		-10	11	-13	13	994	994	13	-13	11	-10	
9		-10	11	-13	13	994	994	13	-13	11	-10	
10		14	-16	23	-27	13	13	-27	23	-16	14	
11					23	-13	-13	23				
12		-10	16		-16	11	11	-16		16	-10	
13			-10		14	-10	-10	14		-10		
14												

FIG. 1. The effect of filtering on a δ function. Fig. 1a shows the result of filtering a δ function of strength 1000 placed in $\bar{\mathbf{x}}=(8,8)$. Fig. 1b shows the effect of filtering on the four δ functions of strength 1000 placed within the heavily drawn 2×2 square in the center of the figure. All values numerically less than 10 have been suppressed.

sented here. Our results will therefore be presented on a 12×12 grid.

The value of $\tau(\bar{\mathbf{x}})$ was determined as described in the previous section with the exception that when $v_1(\bar{\mathbf{x}})$ in (11) is zero, τ is assigned a fairly large value. In the calculations a square mesh was used. The cutoff radius K_f was in all calculations chosen to be $K_f = K_1 = K_2 = \pi$. In the numerical tests the dimensions are chosen such that $\bar{\mathbf{x}}$ is measured in grid units, $\bar{\mathbf{v}}$ in grid units per time unit, τ in time units and D in (grid unit)^2 per time unit. Thus we formally put $\Delta x_1 = \Delta x_2 = 1$. At time t with velocity $\bar{\mathbf{v}}$, a given mass $c(\bar{\mathbf{x}},t)$ will be transported a distance vt. We shall later return to the question of practical units. In numerical tests the term $-\nabla D$ was omitted since for the values of the diffusion constant used, it had no significant effect.

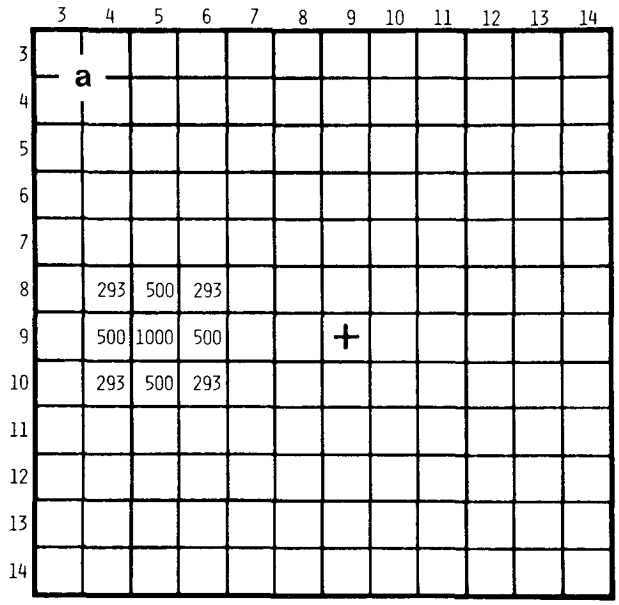

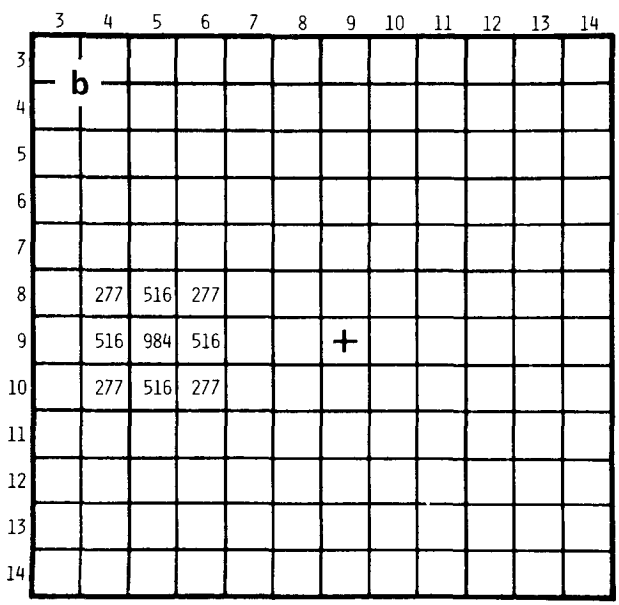

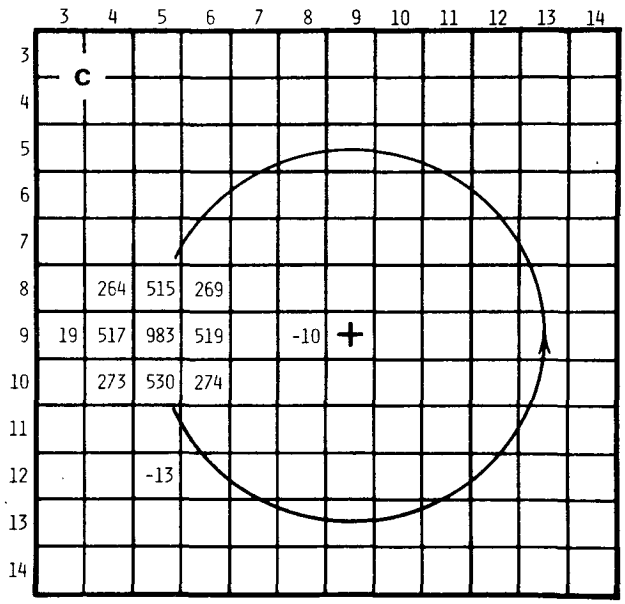

FIG. 2. Representation of a cone of base radius equal to 2 and with an amplitude of 1000 in the center (a), the same after filtering (b), and after one revolution (c) in a uniform circular velocity field centered at $\bar{\mathbf{x}} = (9,9)$. Values numerically less than 10 have been suppressed.

a. Errors introduced by filtering

The pseudospectral method describes advection of the harmonic modes with a high degree of accuracy. The main limitation of the method is the introduction of errors originating from the filtering of the distribution. The largest possible errors are thus created by the filtering of a delta function. Fig. 1a shows a filtered delta function of strength 1000 at $\bar{\mathbf{x}} = (8,8)$. The error decreases with distance from this cell and has a maximum in the nearest neighbor cells of about 15% of the center cell value. The effect of filtering on an arbitrary function is equivalent to a folding of the function in real space with the filtered δ function. An improved resolution is easily obtained by reducing the grid spacing as shown in Fig. 1b, where the single δ function is replaced by four δ functions in neighboring cells, inside the 2×2 square in the center of the figure. The error introduced by filtering is now less than 3% of the cell maximum. Any practical air pollution modeling problem with the exception of point sources will present rather smooth functions and the errors should not exceed a few percent.

b. Advection test

It is important to test the applicability of the pseudospectral method for advection computations. The usual test is a rotation of a conical distribution in a uniform

circular velocity field. The analytical function describing the cone is a distribution $c(\bar{\mathbf{x}},t)$:

$$c(\bar{\mathbf{x}},t=0)=\begin{cases}Q(1-|\bar{\mathbf{x}}'|/r), & |\bar{\mathbf{x}}'|\leqslant r\\ 0, & |x'|>r\end{cases}$$

where $\bar{\mathbf{x}}'=\bar{\mathbf{x}}-\bar{\mathbf{x}}^0$ and where r is the base radius of a cone with a maximum value of Q at the cone center situated in $\bar{\mathbf{x}}^0$. The uniform circular velocity field, centered at $\bar{\mathbf{x}}^*$, is given by $\bar{\mathbf{v}}=\Omega(x_2-x_2^*, -x_1+x_1^*)$. We use $Q=1000$, $r=2$, $\bar{\mathbf{x}}^0=(5,9)$ and $\bar{\mathbf{x}}^*=(9,9)$. These conditions are the same as the ones used by Orszag (1971a). Fig. 2b shows the filtered cone. The error introduced by filtering is only about 1.5% of the value in the cone center. Fig. 2c shows the cone after a rotation of 2π through 800 time steps with filtering at every 50 time step. Generally it was found that less frequent filtering should be combined with a smaller cutoff wavenumber K_f in order to minimize errors. This fits the idea of removing aliasing interactions described in Section 3. The maximum error introduced by the rotation is 2% of the center value, while the loss in the center of the cone is as small as 0.1%.

In Table 1 we have summarized the published results of similar tests with other numerical methods. Max and Min stands for the maximum and the minimum value at any grid point with exact values of 1.00 and 0.00, respectively, as all the cone tests in the table are normalized in this way. Relative computer time is compared only for test between numerical methods given in the same paper. For all methods, sufficiently small time steps are used to avoid errors stemming from the time-integration procedure. The rotating cone test was introduced by Molenkamp (1968) who used a rotation of 0.38π. Later tests were usually performed with a 2π rotation. The base radius of the cone varies. A larger radius gives an improved resolution, and a smaller radius therefore presents a stronger test. The finite difference methods used vary from first order to fourth order in space with improved results and computer time for the higher order methods. For methods based on orthogonal functions such as the Galerkin (spectral) and the pseudospectral method the order in space is infinite in the sense that spatial derivatives contain information about function values on all grid points. If the number of grid points is N, the error goes to zero faster than any power of $1/N$ (Orszag and Israeli, 1974). Methods based on orthogonal functions have the highest accuracy and only slightly increased computation time compared with the fourth-

TABLE 1. Uniform rotation of a cone.

Reference	Method	Order in space	Grid size	Radius of cone	Revolution	Number of time steps	Relative time	Max	Min	Comments
Molenkamp (1968)	Upstream $N+1$	1	25×25	4	0.38π	40	1	0.31	0.00	
	Upstream N	1	25×25	4	0.38π	40	1	0.40	0.00	
	Leap-frog	2	50×50	4	0.38π	40	0.7	0.86	−0.11	
	Lax-Wendroff	2	25×25	4	0.38π	40	1.8	0.75	−0.18	
	Arakawa Euler	2	25×25	4	0.38π	40	1.5	0.86	−0.13	
	Arakawa-Adams-Bashforth	2	25×25	4	0.38π	40	1.6	0.88	−0.13	
	Robert-Weiss	4	50×50	4	0.38π	40	45.0	0.90	−0.02	
Orszag (1971)	Arakawa	2	32×32	2	2.00π	800	1	0.79	−0.13	
	Arakawa	4	32×32	2	2.00π	800	1.6	0.89	−0.05	
	Galerkin(Fourier)	∞	32×32	2	2.00π	800	3.8	0.98	−0.02	
	Galerkin(Fourier)	∞	16×16	2	2.00π	800	0.8	0.97	−0.03	
Fox and Orszag (1973)	Pseudospectral	∞	32×32	2	2.00π	1600		0.98	−0.02	a
Gazdag (1973)	Pseudospectral	∞	32×32	~6	2.00π	400		1.00	0.00	b
Anderson and Fattahi (1974)	Mac Cormack	2	32×32	4	2.00π	200	1	0.60		
	Rusanov	3	32×32	4	2.00π	200	3.0	0.54		
	Kutler-Warming-Lomax	3	32×32	4	2.00π	200	2.6	0.53		
Pedersen and Prahm (1974)	Moment	3		4	0.38π	40		0.81	0.00	c
This study	Pseudospectral	∞	16×16	2	2.00π	800		0.98	−0.01	d
Purnell (1976)	Cubic Spline	3	32×32	4	2.00π	60		0.82		

a: Pseudospectral methods, at least a factor 2 faster than spectral methods.
b: Initial distribution Gaussian and not a cone, thus not directly comparable. Third-order time integration method.
c: Subgrid-scale information possible.
d: Filtering every 50 time steps, enabling solutions in physical space with nonperiodic boundaries. Maximum value is relative to unfiltered cone, maximum value relative to filtered cone is 1.00.

order finite difference Arakawa methods (Orszag, 1971a). Pseudospectral methods are about a factor of 2 more efficient than the spectral methods (Fox and Orszag, 1973). The pseudospectral method given by Gazdag (1973) uses a Gaussian distribution as initial value and is not directly comparable with the other tests. In contrast to other spectral and pseudospectral methods this method does not demand periodic boundary conditions of the *physical* problem considered. Our method is therefore specially applicable for solution of *physical* problems involving transport of pollutants in fluids and gases. The present model thus combines practical applicability with an accuracy as good as in the best numerical methods presently available (Table 1).

c. *Plume test*

Most pollutant sources have a continuous emission during a certain time. Numerical methods describing dispersion of pollutants should thus be able to reproduce a continuous source sufficiently accurately. Fig. 3a shows the exact solution to the concentration from six continuous sources each with a source strength $Q=100$ mass units per grid cell per time unit in the homogeneous wind field $\bar{\mathbf{v}}=(1,1)$. The derivation of this result is discussed in the following section. Our pseudospectral method is able to reproduce this with typical errors of about 5% of the maximum value in the area (Fig. 3b). Although the emission has taken place during a time corresponding to a travel distance twice through the grid system, no pollution reappears on the grid system after being advected out over the boundary. This example shows that the idea of introducing a drain term at the boundary in order to override periodic boundary conditions works in practice. As a second example of this we have tested advection of the conical distribution of Fig. 2a out over the boundary. The center of the cone was at $\bar{\mathbf{x}}^0=(4,4)$ and a uniform circular velocity field was centered at $\bar{\mathbf{x}}^*=(13,4)$. The conical distribution then passes the boundary after rotating more than $\pi/2$. After rotating an angle of π, the maximum numerical value at a grid point was 0.4% of the initial cone maximum. This example further confirms the choice of decay time given in (11).

In Fig. 4 is shown a numerical test with a plume subject to both advection $[\bar{\mathbf{v}}=(0,1)]$ and diffusion $(D=0.1)$. The plume originates from four continuous adjacent sources each of source strength $Q=250$ mass units per time unit per cell. The analytical solution, as shown in Fig. 4a, is given by

$$c(x_1,x_2)=\begin{cases}\dfrac{Q}{v_2(2\pi\sigma^2)^{\frac{1}{2}}}\exp(-x_1^2/2\sigma^2), & x_2>0\\[2ex] \dfrac{Q}{2v_2}\delta(x_1), & x_2=0\end{cases}$$

Here $\sigma^2=2Dx_2/v_2$ and on a discrete grid system $\delta(x_1)$ is replaced by $1/\Delta x_1$. The numerical solution in Fig. 4b deviates less than 5% from the analytical solution on grid points more than one grid unit displaced from the source area. This error is mainly due to the fairly course grid system, that is, the analytical solution contains Fourier components with wavelengths too small to be represented on the grid system. The error is reduced when a smaller mesh spacing is used.

5. Discussion

a. *Interpretation of results*

The main difference between the present model and many models used in air pollution studies is that the quantity $c(\bar{\mathbf{x}},t)$ is to be interpreted as the *concentration* in the point $\bar{\mathbf{x}}$ and not as the *mass* of pollutant in a *cell* surrounding $\bar{\mathbf{x}}$.

Problems with interpretation do only arise in the case where $c(\bar{\mathbf{x}},t)$ is not a smooth function but has the character of a δ function. This is particularly the case for the values of $c(\bar{\mathbf{x}},t)$ at grid points in the neighborhood of a source when diffusion is present or for the values of $c(\bar{\mathbf{x}},t)$ on points downwind of the source in the case of pure advection.

These features are best illustrated for the case of a homogeneous velocity field and with only a single source present. We shall furthermore assume a steady-state situation. We choose a grid coordinate x_2^0 downwind from the source, and let the velocity be $\bar{\mathbf{v}}=(v_1,v_2)$. For $\bar{\mathbf{x}}$ continuous the continuity equation yields

$$\int_{-\infty}^{\infty} v_2 c(x_1,x_2^0)dx_1=Q,$$

which on the grid system is replaced by

$$v_2\sum_{x1} c(x_1,x_2^0)\Delta x_1\approx Q. \tag{14}$$

In numerical tests the last relation was found to hold within few percent. In the units we use here $\Delta x_1=\Delta x_2=1$.

For an arbitrary direction of velocity it is not in general possible to predict values of $c(\bar{\mathbf{x}})$ on grid points since $c(\bar{\mathbf{x}})$ has the character of a δ function and is therefore only defined through integral properties as stated in Eq. (14). There are two special cases of this rule, however, namely for v_1 or v_2 equal to zero and for v_1 equal to v_2. In both cases $c(\bar{\mathbf{x}})$ is zero on grid points except in the downwind direction from the source. When $\bar{\mathbf{v}}=(0,v)$ the non-zero values can be found from (14) as $c=Q/v$. When $\bar{\mathbf{v}}=2^{\frac{1}{2}}v(\frac{1}{2},\frac{1}{2})$ the value becomes $c=2^{\frac{1}{2}}Q/v$. This difference indicates that a source should be interpreted as an *area* source since the concentration is proportional to length in a unit cell swept by the wind. The last example explains the theoretical result of Fig. 3a. When several adjacent sources are present it

was found that the concentration profile for constant x_1 or x_2 fitted the continuous profile calculated by considering the sources as area sources. Although this is a consistent interpretation it should be mentioned that it is a consequence of the discrete grid system together with the continuity equation since the method does not distinguish between a point source and an area source on a discrete grid. If we consider the two above mentioned examples in the case of a nonzero

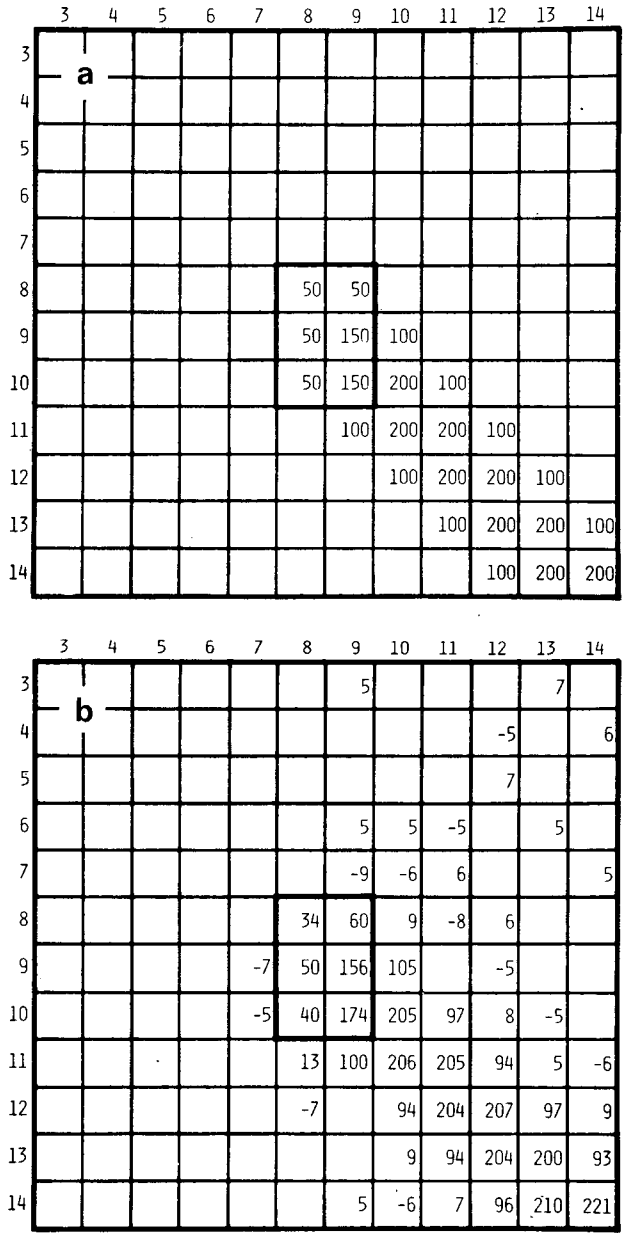

FIG. 3. Result of advection from six sources placed within the heavily drawn rectangle. Each source has the strength 100. The velocity field is homogeneous with $\bar{v}=(1,1)$. Theoretical result (a) and numerical result (b) obtained in steady state, i.e., at time 32 corresponding to advection of a given point twice through the grid system. There is no essential change in the result from $t=8$ to $t=32$. Values numerically less than 5 have been suppressed.

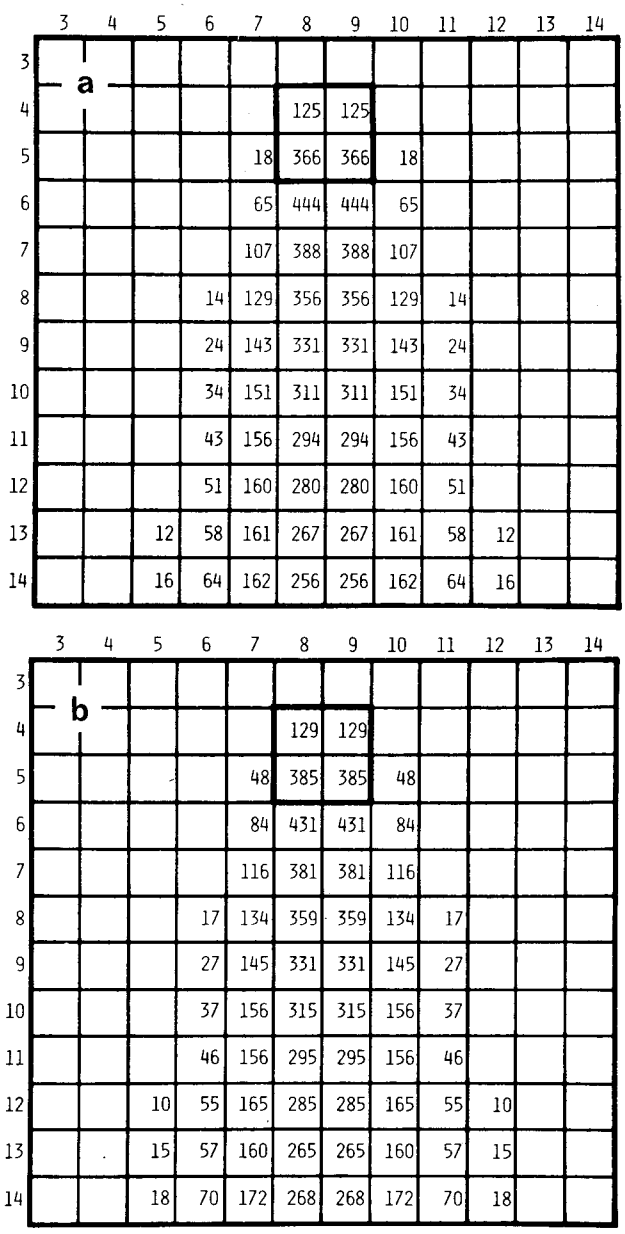

FIG. 4. Test with simultaneous advection and diffusion from four sources placed within the heavily drawn square. Each source has the strength 250. The velocity field is homogeneous with a value $\bar{v}=(0,1)$. The diffusion constant is equal to 0.1. Theoretical result (a) and numerical steady-state result (b) after $t=32$ corresponding to advection of a point twice through the grid system. There is no essential change in the result from $t=16$ to $t=32$. Values numerically less than 10 have been suppressed.

diffusion constant we find that the concentration is independent of the direction of velocity except close to the source where diffusion has little effect on the result.

b. Applications to air pollution modeling

It is of interest for air pollution modeling to estimate the computer time necessary to perform a computation

of air pollution concentration on a given scale. We choose the grid spacing L(m) as the distance unit and time unit T(s). We can then introduce the dimensionless quantities $\bar{\mathbf{x}}'$ and t' where $\bar{\mathbf{x}}=\bar{\mathbf{x}}'L$ and $t=t'T$. Substituting these expressions in the dispersion equation (1) we obtain

$$\frac{\partial c}{\partial t'}=-\bar{v}'\cdot\nabla' c+\nabla'\cdot(D'\nabla' c)-\frac{c}{\tau'}+Q', \qquad (15)$$

where $\bar{v}'=\bar{v}(T/L)$, $D'=D(T/L^2)$, $\tau'=\tau/T$, $Q'=Q\cdot T$, and where ∇' is the derivative with respect to the spatial variable $\bar{\mathbf{x}}'$. The primed quantities are dimensionless variables which permit a direct comparison between actual physical parameters and the ones used in the numerical tests. Usually Q is specified in, say, kilograms per grid cell per second and c will then be found in units of kilograms per grid cell. In order for time integration errors to be negligible we require that $v'_{\max}\Delta T'\leqslant 0.1$, where $\Delta T'$ is the dimensionless time step. For a given grid size these relations permit us to find dimensionless parameters and to relate computation time to real time. Such a comparison is made in Table 2 for grid spacings of 10 and 100 km. The computer time per time step on a 32×32 grid is $\sim$0.7 s. No special efforts were made to save computer time. Because of the fast Fourier transform algorithm, the concentration was evaluated as a complex quantity with zero imaginary part. This can be used advantageously to handle two concentrations at the same time which is desirable, for instance, in modeling simultaneous concentrations of SO_2 and $SO_4^=$. In the present study, computer time could be halved by introducing a real fast Fourier Transform algorithm. Thus real times corresponding to the 1000 time steps in Table 2 would require approximately 6 min of computer time.

In Table 2 we have chosen an average wind velocity of 10 m s^{-1} and a diffusion constant of 1000 m^2 s^{-1} as estimated from the horizontal spread of a plume 10 km from the source under very unstable atmospheric weather conditions (Pasquill, 1974). The effect of horizontal diffusion is to transform a δ function into a Gaussian distribution with a standard deviation of $(2DT)^{\frac{1}{2}}$ at time T. The maximum time of relevance here is the travel time through the grid system. The corresponding standard deviation is given in Table 2. On a regional scale ($L=100$ km) the effect of diffusion can be neglected. The actual "diffusion" which takes place here is due to variation of wind direction on a synoptic scale. This shows the importance of using a numerical model which is free of pseudo-diffusion effects. On a mesoscale ($L=10$ km) horizontal diffusion should probably still be taken into account, particularly during unstable atmospheric weather conditions.

TABLE 2. Typical orders of magnitude for air pollution modeling.

Geographical scale	Mesoscale	Regional
Grid spacing L(km)	10	100
Dimensionless velocity v'	3.6	0.36
Real time corresponding to 1000 time steps	30	300
Dimensionless diffusion constant D'	3.6×10^{-2}	3.6×10^{-4}
Travel time through 32 grid cells T'	9	90
Standard deviation $(2D'T')^{\frac{1}{2}}$	$0.8L$	$0.25L$

$v=10$ m s^{-1}, $D=1000$ m^2 s^{-1}, time unit $T=1$ h.

6. Conclusions

The purpose of this paper has been to develop an accurate numerical model to solve the dispersion equation. The model is based on the pseudospectral method. This is presently the best numerical integration method available with respect to accuracy and computation time. In order to obtain a model with realistic boundary conditions we have introduced a drain term at the grid boundary. A filtering procedure prevents errors due to aliasing interactions. The errors introduced by filtering are negligible in most practical cases. To our knowledge the present model is the most accurate Eulerian model currently available for practical dispersion calculations in fluids and gases.

The main objective has been to present numerical documentation relevant to air pollution studies. Applications of the model to such problems is only limited by the validity of the gradient transfer theory. Typical examples of future applications is the study of dispersion of pollutants on a regional scale and on the mesoscale. Transport of anthropogen pollution on a regional scale has been reported by Prahm *et al.* (1974, 1976) and regional modelling is currently performed for the European area (Ottar, 1973; Eliassen and Saltbones, 1975b; Nordlund, 1975).

Acknowledgments. We would like to thank Per G. Thomsen, Technical University of Denmark, for stimulating discussions and Steven A. Orszag, Massachusetts Institute of Technology, for an enlightening correspondence.

This research was initiated as a part of the project "Mesoscale Modelling" organized by the Scandinavian Council for Applied Research, and the study was supported by the Danish Technical Scientific Research Foundation.

REFERENCES

Anderson, D., and B. Fattahi, 1974: A comparison of numerical solutions of the advective equation. *J. Atmos. Sci.*, **31**, 1500–1506.

Christensen, O., and L. P. Prahm, 1976: A pseudospectral model for dispersion of atmospheric pollutants: Computer program. Report, Danish Meteorological Institute.

Cooley, J. W., and J. W. Tukey, 1965: An algorithm for the machine calculation of complex Fourier series. *Math. Comput.*, **19**, 297–301.

Crowley, W. P., 1968: Numerical advection experiments. *Mon. Wea. Rev.*, **96**, 1–11.

Egan, B. A., and J. R. Mahoney, 1972a: Numerical modeling of advection and diffusion of urban area source pollutants. *J. Appl. Meteor.*, **11**, 312–322.

——, and ——, 1972b: Applications of a numerical air pollution transport model to dispersion in the atmospheric boundary layer. *J. Appl. Meteor.*, **11**, 1023–1039.

Eliassen, A., and J. Saltbones, 1975a: A two-layer dispersion model, description and a few results. Rep. LRTAP 5/75, Norwegian Institute for Air Research, Kjeller.

Eliassen, A., and J. Saltbones, 1975b: Decay and transformation rates of SO_2 as estimated from emission data, trajectories and measured air concentrations. *Atmos. Environ.*, **9**, 425–429.

Fox, D. G., and S. A. Orszag, 1973: Pseudospectral approximation to two-dimensional turbulence. *J. Comput. Phys.*, **11**, 612–619.

Galerkin B. G., 1915: Series occurring in some problems of elastic stability of rods and plates. *Eng. Bull.*, **19**, 897–908.

Gazdag, J., 1973: Numerical convective schemes based on accurate computation of space derivatives. *J. Comput. Phys.*, **13**, 100–113.

Lambert, J. D., 1973: *Computational Methods in Ordinary Differential Equations*. Wiley, 44 pp.

Lanczos, C., 1957: *Applied Analysis*. Prentice-Hall.

Molenkamp, C. R., 1968: Accuracy of finite-difference methods applied to the advection equation. *J. Appl. Meteor.*, **7**, 160–167.

Monin, A. S., and A. M. Yaglom, 1971: *Statistical Fluid Mechanics: Mechanics of Turbulence*. The MIT press, 579 pp.

Nordlund, G. G., 1975: A quasi-Lagrangian cell method for calculating long-distance transport of airborne pollutants. *J. Appl. Meteor.*, **14**, 1095–1104.

Orszag, S. A., 1971a: Numerical simulation of incompressible flows within simple boundaries: accuracy. *J. Fluid Mech.*, **49**, part 1, 75–112.

——, 1971b: Numerical simulation of incompressible flows within simple boundaries. I. Galerkin (spectral) representations. *Stud. Appl. Math.*, **50**, 293–326.

——, and M. Israeli, 1974: Numerical simulation of viscous incompressible flows. *Annual Reviews Fluid Mechanics*, Vol. 6, 281–317.

Ottar, B., 1973: The long range transport of air pollutants. *Proc. Third Intern. Clean Air Congress*, Düsseldorf, B102–B104.

Pasquill, F., 1974: *Atmospheric Diffusion*. Wiley.

Pedersen, L. B., and L. P. Prahm, 1974: A method for numerical solution of the advection equation. *Tellus*, **26**, 594–602.

Phillips, N. A., 1959: An example of non-linear computational instability. *The Atmosphere and the Sea in Motion*, Oxford University Press, 501–505.

Prahm, L. P., H. S. Buch and U. Torp, 1974: Long range transport of atmospheric pollutants over the Atlantic. *Preprints Symp. Atmospheric Diffusion and Air Pollution*. Santa Barbara, Amer. Meteor. Soc., 190–195.

——, U. Torp and R. M. Stern, 1976: Deposition and transformation rates of sulphur oxides during atmospheric transport over the Atlantic. *Tellus*, **28**, 355–372.

Purnell, D. K., 1976: Solution of advective equation by upstream interpolation with a cubic spline. *Mon. Wea. Rev.*, **104**, 42–48.

Sheih, C. M., and W. J. Moroz, 1973: A Lagrangian puff diffusion model for the prediction of pollutant concentrations over urban areas. *Proc. Third Intern. Clean Air Congress*, Düsseldorf, B43–B52.

Sklarew, R. C., A. J. Fabrick and J. E. Prager, 1971: A particle-in-cell method for numerical solution of the atmospheric diffusion equation, and applications to air pollution problems. Rep. 3SR-844, Vol. 1, *Systems, Science and Software*, La Jolla, Calif.

Start, G. E., and L. L. Wendell, 1974: Regional effluent dispersion calculations considering spatial and temporal meteorological variations. *Preprints Symp. Atmospheric Diffusion and Air Pollution*. Santa Barbara, Amer. Meteor. Soc., 202–208.

Taylor, G. I., 1921: Diffusion by continuous movements. *Proc. London Math. Soc.*, Ser. 2, **20**, 196–213.